SANDIA REPORT

SAND2018-3623
Unlimited Release
Printed Sept 2017

Development of harmonic balance capability for Charon

Andy C. Huang

Prepared by
Sandia National Laboratories
Albuquerque, New Mexico 87185 and Livermore, California 94550

Sandia National Laboratories is a multimission laboratory managed and operated by National Technology and Engineering Solutions of Sandia, LLC., a wholly owned subsidiary of Honeywell International, Inc., for the U.S. Department of Energys National Nuclear Security Administration under contract DE-NA0003525.

Approved for public release; further dissemination unlimited.

Reviewed by: Lawrence C Musson ____
Date: 05 September 2017

Sandia National Laboratories

Issued by Sandia National Laboratories, operated for the United States Department of Energy by National Technology and Engineering Solutions of Sandia, LLC.

SAND2018-3623
Unlimited Release
Printed Sept 2017

Development of harmonic balance capability for Charon

Andy C. Huang
Electrical Models and Simulation
Sandia National Laboratories
P.O. Box 5800
Albuquerque, NM 87185-9999
ahuang@sandia.gov
MS 1177

Abstract

We report on the development of a frequency domain method of analysis in the Panzer foundation of Charon.

We first present a harmonic balance approach for calculating the frequency-domain response (in its weak form) of a non-linear system of partial differential equations (PDEs). Our approach is anemable to adaptation of Charon's transient PDE models for frequency domain analysis. We make an observation that allows us to analyze either small-signal or large-signal responses with minimal specialization of the algorithm.

We conclude by confirming our small- and large-signal analyses of a transient, linear Helmholtz equation by comparing its analytic solution to our results. We include figures from a sequence of non-linear perturbations of this system, showcasing the fact that, when the non-linearities are insignificant, the small- and large-signal analyses obtain similar solutions. On the other hand, we depict the inadequacy of a small-signal analysis to accurately capture the response in the presence of a large non-linearity, and underscore the requirement to employ a large-signal analysis for modelling highly non-linear systems.

Acknowledgment

The author would like the especially thank the Charon team - Suzey Gao, Gary Hennigan, Larry Musson, and Mihai Negoita - for their encouragement and guidance. They have all been excellent buddies and mentors. Thanks are also due to many Trilinos developers from whom the author has shared patient, helpful, and insightful conversations: Eric Phipps, Roger Pawlowski, Eric Cyr, Stephen Bond, Kara Peterson, and Jason Gates.

Contents

Figures

This page intentionally left blank.

1 Notation

We consider a parabolic PDE

$$\frac{\partial u}{\partial t} = \mathcal{F}(u(x,t), f(x,t))$$

on a compact domain $D \subset \mathbb{R}^3$, where $f(x,t)$ is a quasi-periodic function whose spectrum is supported at positive integer linear combinations of *stimulus frequencies* $0 < \omega_1 < \ldots < \omega_M$ for $M \in \mathbb{N}$. Any boundary conditions are assumed to be band-limited to this same set of frequencies. We seek its solution $u(x,t)$. Under reasonable conditions on $\mathcal{F}$, the solution $u(x,t)$ is itself a quasi-periodic function.

Denote the *vector of stimulus frequencies* by $\vec{\omega} = (\omega_1, \ldots, \omega_M)$. A harmonic balance method adopts $\vec{\omega}$ into a *truncation scheme* $\mathcal{T} \subsetneq \mathbb{Z}^M$ which indexes integer linear combinations of the stimulus frequencies faithfully, i.e. $|\mathcal{T}| = |\vec{\omega} \cdot \mathcal{T}|$, and which supports the spectrum of f. The truncation scheme dictates the *truncated frequency basis* $\Omega := \vec{\omega} \cdot \mathcal{T}$. Our harmonic balance assumes the solution ansatz

$$u(x,t) = U_0(x) + \sum_{\alpha \in \mathcal{T}} \left[U^c_{\vec{\alpha}}(x) \cos(\vec{\alpha} \cdot \vec{\omega} t) + U^s_{\vec{\alpha}}(x) \sin(\vec{\alpha} \cdot \vec{\omega} t) \right].$$

We express f in the corresponding form, following the truncation scheme, as

$$f(x,t) = F_0(x) + \sum_{\vec{\alpha} \in \mathcal{T}} \left[F^c_{\vec{\alpha}}(x) \cos(\vec{\alpha} \cdot \vec{\omega} t) + F^s_{\vec{\alpha}}(x) \sin(\vec{\alpha} \cdot \vec{\omega} t) \right].$$

We call $P := max_{\vec{\alpha} \in \mathcal{T}} ||\vec{\alpha}||_{\ell^\infty}$ the *order of the truncation scheme*, and $H := |\mathcal{T}|$ the *total number of harmonics* of the truncation scheme. We introduce an ordering $\succ$ on $\mathcal{T}$ so that $\vec{\alpha} \succ \vec{\beta}$ if and only if $\vec{\alpha} \cdot \vec{\omega} > \vec{\beta} \cdot \vec{\omega}$; note that $|\Omega| = 2M + 1$, accounting for the cosine, sine, and constant terms.

2 Mathematical description of harmonic balance approach

A successful harmonic balance method first determines a system of equations whose degrees of freedom are the coefficients of the solution ansatz, $\{U_0(x), U^c_k(x), U^s_k(x) | k = 1, \ldots, 2H\}$, and then solves this system to determine these coefficients. In the weak form, this amounts to minimizing the residuals coming from projecting $(\mathcal{F} - \partial_t)(u)$ onto a space of spatial-temporal test functions. In this section, we focus on obtaining this system of harmonic balance equations.

Let $\{x_n\}$ be the set of nodal points of a mesh $M \subset D$, and let $\{\phi_n | x_n \in M\}$ be the set of nodal basis functions. Our set of spatial-temporal space of test functions is given by

$$\{\phi_n \otimes 1, \phi_n \otimes \cos(2\pi\omega_k t), \phi_n \otimes \sin(2\pi\omega_k t) | x_n \in D, \omega_k \in \Omega\}.$$

Hence, the system of residual equations is, for all admissible n and k:

$$0 = \int_{t=0}^{t=1} \int_V \left[\left(\mathcal{F} - \partial_t \right)(u) \right] \cdot \phi_n \cdot 1 \, dx \, dt$$
$$0 = \int_{t=0}^{t=1} \int_V \left[\left(\mathcal{F} - \partial_t \right)(u) \right] \cdot \phi_n \cdot cos(2\pi\omega_k t) \, dx \, dt$$
$$0 = \int_{t=0}^{t=1} \int_V \left[\left(\mathcal{F} - \partial_t \right)(u) \right] \cdot \phi_n \cdot sin(2\pi\omega_k t) \, dx \, dt$$

Let the right-hand sides of these equations be denoted by $\mathcal{R}_0, \mathcal{R}^C_{\omega_k}, \mathcal{R}^S_{\omega_k}$, respectively. Note that $\mathcal{R}^C_{\omega_k}$ is nothing other than a (spatially integrated) Fourier coefficient of $(\mathcal{F} - \partial_t)\, u$, so the harmonic balance method essentially drives the frequency domain response of the system to 0.

For example, fix $\omega_k \in \Omega$; for each nodal basis function ϕ_n (having support in $V \subset D$) we obtain:

$$\begin{aligned}
\mathcal{R}^C_{\omega_k}\left(U_0, U^C_{\omega_j}, U^S_{\omega_j}\right) &= \langle \mathcal{F}(u) - \partial_t u, \phi_n(x,y) \otimes cos\left(2\pi\omega_k t\right) \rangle_{\mathcal{L}^2(V \times [0,1])} \\
&= \int_{t=0}^{t=1} \int_V \mathcal{F}(u(x,y,t)) \cdot \phi_n(x,y) \cdot \cos(2\pi\omega_k t) \, dvol_V \, dt \qquad \text{by linearity} \\
&\qquad - \int_{t=0}^{t=1} \int_V \partial_t u \cdot \phi_n(x,y) \cdot \cos\left(2\pi\omega_k t\right) dvol_V \, dt \\
&\approx \sum_{i=0}^{L} \left[\int_V \mathcal{F}(u(x,y,t_i)) \cdot \phi_n(x,y) \, dvol_V \right] w_i \cos(2\pi\omega_k t_i) \qquad \text{by quadrature in } dt \\
&\qquad + 2\pi\omega_k \int_{t=0}^{t=1} \int_V u(x,y,t) \cdot \phi_n(x,y) \cdot \sin\left(2\pi\omega_k t\right) dvol_V \, dt \qquad \text{by IBP in } t \\
&\approx \sum_{i=0}^{L} \left[\int_V \mathcal{F}(u(x,y,t_i)) \cdot \phi_n(x,y) \, dvol_V \right] w_i \cos(2\pi\omega_k t_i) \\
&\qquad + 2\pi\omega_k \frac{1}{2} \int_V U^S_{\omega_k} \cdot \phi_n(x,y) \, dvol_V \quad \text{since } \int_{t=0}^{t=1} u(t) \cdot \sin\left(2\pi\omega_k t\right) dt = \frac{1}{2} U^S_{\omega_k}
\end{aligned}$$

where $w_i = \frac{1}{2}$ if $i = 0, L$ or else $w_i = 1$ (for the trapezoidal rule). Note that

$$\mathcal{R}_{TD}(u(t_i), \phi_n) := \left[\int_V \mathcal{F}(u(x,y,t_i)) \cdot \phi_n(x,y) \, dvol_V \right]$$

is a residual equation calculated by a transient simulation, say, at each time step in a backward Euler method of analysis.

3 Implementation of approach

We arrive at the following process for calculating the harmonic balance residuals $\mathcal{R}_0, \mathcal{R}^C_{\omega_k}, \mathcal{R}^S_{\omega_k}$:

1. For each $i = 0, \ldots, L$, set up the frequency domain degrees of freedom U_0, U_k^C, U_k^S:

$$u(t_i) = U_0 \cdot 1 + \sum_{\omega_k \in \Omega} \left[U^c_{\omega_k} \cdot \cos(2\pi\omega_k t_i) + U^s_{\omega_k} \cdot \sin(2\pi\omega_k t_i) \right]$$

2. Calculate the time domain residual

$$\mathcal{R}_{TD}(u(t_i), \phi_n) := \int_V \mathcal{F}(u(x,y,t_i)) \cdot \phi_n(x,y)\, dvol_V$$

3. Combine the time domain residuals and the $\frac{\partial u}{\partial t}$ residual to form

$$\mathcal{R}^C_{\omega_k} = \sum_{i=0}^{L} \mathcal{R}_{TD}(u(t_i), \phi_n) \cdot w_i \cdot \cos(2\pi\omega_k t_i) + \pi\omega_k \int_V U^S_{\omega_k} \cdot \phi_n(x,y)\, dvol_V$$

We present this process as an algorithm:

Initialize FD residual: $\mathcal{R}^C_{\omega_k} = \pi\omega_k \langle U^S_{\omega_k}, \phi_n \rangle_{\mathcal{L}^2(V)}$

$$\left.\begin{array}{l} \text{Determine DOF at } t_i\text{: } u(t_i) = U_0 + \sum_{k=0}^{M} \left[U^C_{\omega_k} \cos(\omega_k 2\pi t_i) + U^S_{\omega_k} \sin(\omega_k 2\pi t_i) \right] \\ \text{Contribute } t_i \text{ TD residual: } \mathcal{R}^C_{\omega_k} += \mathcal{R}_{TD}(u(t_i), \phi_n) \cdot w_i \cdot \cos(2\pi\omega_k t_i) \end{array}\right\}$$

where we perform the steps outlined by the brace for each t_i, for $i = 0, \ldots, L$. We refer to these steps as the Initialize, DOF(t_i), and Update(t_i) steps. Note that the number of time integration points should be at least $2\max\{|\omega_k|\}$, by the Nyquist Sampling Theorem, i.e., $L = 2\omega_M$. These frequencies may be large, so we remap the frequencies.

3.1 Incorporation of small-signal analyses

The preceding discussion presented an algorithm for performing a large-signal analysis, capturing non-linear interactions between the stimulus harmonics according to the truncation scheme. In this section, we consider a modification of the preceding algorithm to achieve a small-signal analysis.

The small-signal approximation is that superposition applies: *for each $0 \leq k \leq H$, only the $U^C_{\omega_k} \cos(\omega_k 2\pi t)$ and $U^S_{\omega_k} \sin(\omega_k 2\pi t)$ terms of the degree of freedom contribute to $\mathcal{R}^C_{\omega_k}$ and $\mathcal{R}^S_{\omega_k}$, and these degrees of freedom interact only at the first order*. In symbols, this amounts to

$$\mathcal{F}\left(U_0 + \sum_{k=0}^{H} \left[U^C_{\omega_k} \cos(\omega_k 2\pi t) + U^S_{\omega_k} \sin(\omega_k 2\pi t) \right] \right)$$
$$\approx \mathcal{F}(U_0) + \sum_{k=0}^{H} \left[\mathcal{F}\left(U^C_{\omega_k} \cos(\omega_k 2\pi t) \right) + \mathcal{F}\left(U^S_{\omega_k} \sin(\omega_k 2\pi t) \right) \right]$$

Including the temporal derivative, this means that the PDE decouples to become:

$$
\begin{aligned}
(\mathcal{F}-\partial_t)(u) &= (\mathcal{F}-\partial_t)\left(\sum_{k=0}^{H}\left[U^C_{\omega_k}\cos(\omega 2\pi t)+U^S_{\omega_k}\sin(\omega_k 2\pi t)\right]\right)\\
&\approx \sum_{k=0}^{H}\left[(\mathcal{F}-\partial_t)\left(U^C_{\omega_k}\cos(\omega 2\pi t)+U^S_{\omega_k}\sin(\omega_k 2\pi t)\right)\right]\\
&\approx \sum_{k=0}^{H}\left[(\mathcal{F}-\partial_t)\left(U^C_{\omega_k}\cos(\omega 2\pi t)\right)+(\mathcal{F}-\partial_t)\left(U^S_{\omega_k}\sin(\omega_k 2\pi t)\right)\right]\\
&\approx \sum_{k=0}^{H}\left[\mathcal{F}\left(U^C_{\omega_k}\cos(\omega 2\pi t)\right)+U^C_{\omega_k}\sin(\omega_k 2\pi t)+\mathcal{F}\left(U^S_{\omega_k}\sin(\omega_k 2\pi t)\right)-U^S_{\omega_k}\cos(\omega_k 2\pi t)\right]
\end{aligned}
$$

By letting t_i index an equation - and not time - we can modify an implementation of the large-signal method to instead capture the small-signal response by applying this mathematical assumption. Consider the following modification to the steps above for determining the cosine residual equations (denoting the large-signal and small-signal procedures by LS and SS):

$$
\begin{aligned}
&\text{LS Initialize: } \mathcal{R}^C_{\omega_k} &= \;& \pi\omega_k\langle U^S_{\omega_k},\phi_n\rangle_{\mathcal{L}^2(V)}\\
&\text{SS Initialize: } \mathcal{R}^C_{\omega_k} &= \;& \pi\omega_k\langle U^S_{\omega_k},\phi_n\rangle_{\mathcal{L}^2(V)}
\end{aligned}
$$

$$
\begin{aligned}
&\text{LS DOF}(t_i)\text{: } u(t_i) &= \;& U_0\cdot 1 + U^C_{\omega_1}\cdot\cos(\omega_1 2\pi t_i) + U^S_{\omega_1}\cdot\sin(\omega_1 2\pi t_i) + \cdots\\
&\text{SS DOF}(t_i)\text{: } u(t_i) &= \;& U_0\cdot\delta_{i0} + U^C_{\omega_1}\cdot\delta_{i1}\cdot cos(\omega_1 2\pi t) + U^S_{\omega_1}\cdot 0 + \cdots
\end{aligned}
$$

$$
\begin{aligned}
&\text{LS Update}(t_i)\text{: } \mathcal{R}^C_{\omega_k} \mathrel{+}= \mathcal{R}_{TD}(u(t_i))\cdot w_i\cdot\cos(\omega_k 2\pi t_i)\\
&\text{SS Update}(t_i)\text{: } \mathcal{R}^C_{\omega_k} \mathrel{+}= \mathcal{R}_{TD}(u(t_i))\cdot\delta_{ik}\cdot w_i\cos(\omega_k 2\pi t_i)
\end{aligned}
$$

where δ_{ik} is the Kronecker delta symbol, equal to 1 when $i=k$ and equal to 0 otherwise (and where $w_i=1$ for $i=0,L$ and $w_i=\frac{1}{2}$ otherwise, as before). As i ranges through $0,\ldots,L$, we loop through the DOF(t_i) and Update(t_i) steps. For the large-signal analysis, L is determined by the truncation scheme, and is at least that suggested by the Nyquist Sampling Theorem. For the small-signal analysis, we have $L=2H-1$ (the number of constant, cosine, and sine terms) residual equations.

For example, $k=1$ yields $\mathcal{F}(u(t_i))=\mathcal{F}\left(U^C_1\cos(\omega_k 2\pi t_i)\right)$, so that $\mathcal{F}$ only depends on $U^C_{\omega_1}$:

$$
\therefore \mathcal{R}^C_{\omega_1}\left(U^C_{\omega_1},U^S_{\omega_1}\right)=\pi\omega\left\langle U^S_{\omega_1},\phi_n\right\rangle_{\mathcal{L}^2(V)}+\int_{t=0}^{t=1}\mathcal{R}_{TD}\left(U^C_{\omega_1}\cos(\omega_1 2\pi t)\right)\cdot\cos(\omega_1 2\pi t)\,dt
$$

Hence, this method applies the assumption that the harmonic $\cos(\omega_1 2\pi t)$ only interacts with $\sin(\omega_1 2\pi t)$, and no other harmonics, *to the first order*. Non-linear terms introduce cross-harmonic interactions, and are not included. In this sense, only the truncation coefficient vectors which are

0 in the components for $\omega_2, \ldots, \omega_M$ are captured. We present the algorithm for the sine residual equations for completeness:

$$\begin{aligned}
\text{LS Initialize: } \mathcal{R}^S_{\omega_k} &= \pi\omega_k \langle U^C_{\omega_k}, \phi_n \rangle_{\mathcal{L}^2(V)} \\
\text{SS Initialize: } \mathcal{R}^S_{\omega_k} &= \pi\omega_k \langle U^C_{\omega_k}, \phi_n \rangle_{\mathcal{L}^2(V)}
\end{aligned}$$

$$\begin{aligned}
\text{LS DOF}(t_i)\text{: } u(t_i) &= U_0 \cdot 1 + U^C_{\omega_1} \cdot \cos(\omega_1 2\pi t_i) + U^S_{\omega_1} \cdot \sin(\omega_1 2\pi t_i) + \cdots \\
\text{SS DOF}(t_i)\text{: } u(t_i) &= U_0 \cdot \delta_{i0} + U^C_{\omega_1} \cdot 0 + U^S_{\omega_1} \cdot \delta_{i1} \cdot \sin(\omega_1 2\pi t) + \cdots
\end{aligned}$$

$$\begin{aligned}
\text{LS Update}(t_i)\text{: } \mathcal{R}^C_{\omega_k} &\mathrel{+}= \mathcal{R}_{TD}(u(t_i)) \cdot w_i \cdot \sin(\omega_k 2\pi t_i) \\
\text{SS Update}(t_i)\text{: } \mathcal{R}^C_{\omega_k} &\mathrel{+}= \mathcal{R}_{TD}(u(t_i)) \cdot \delta_{ik} \cdot w_i \cdot \sin(\omega_k 2\pi t_i)
\end{aligned}$$

4 Validation

When it is known a priori that the solution u is band limited, then a reasonable implementation of the harmonic balance method with a truncated frequency basis containing the frequency spectrum of u should recover u. In this section, we verify our method on a linear PDE with a band-limited analytic solution. We then also present the results of a non-linear perturbation of that simple system.

4.1 Solution of a linear transient Helmholtz problem

Consider the PDE

$$\frac{\partial u}{\partial t} = \mathcal{F}(u(x,t)) = u_{xx} \text{ on the domain } \left[0, 2\sqrt{\pi}\right] \times \mathbb{S}^1$$

with Dirichlet boundary conditions

$$\begin{aligned}
u(0,t) &= \sin(2\pi t) \\
u\left(2\sqrt{\pi}, t\right) &= e^{-2\pi} \sin(2\pi t)
\end{aligned}$$

where $\mathbb{S}^1$ is simply the interval $[0, 2\pi]$ with the endpoints identified. This is equivalent to considering the same PDE on $[0, 2\pi] \times \mathbb{R}$ while demanding $2\pi-$periodicity of the solution, i.e., $u(x,t) = u(x, t + 2\pi)$ for all $t \in \mathbb{R}$. The PDE admits an exact travelling wave solution:

$$u(x,t) = e^{-\sqrt{\pi}x} \sin\left(2\pi t - \sqrt{\pi}x\right)$$

Note that this analytic solution can be expressed in the space-frequency domain as:

$$u(x,t) \equiv -e^{-\sqrt{\pi}x} \sin(\sqrt{\pi}x) \cos(2\pi t) + e^{-\sqrt{\pi}x} \cos(\sqrt{\pi}x) \sin(2\pi t)$$

In Figure 1, we present the result of our large- and small-signal simulations of this linear transient Helmholtz problem alongside the analytic solution. The numerical solution takes the form

$$U(x,t) = U^C_{\omega_1}(x) \cos(2\pi t) + U^S_{\omega_1}(x) \sin(2\pi t)$$

and our harmonic balance method seeks to determine the coefficient functions $U^C_{\omega_1}(x)$ and $U^S_{\omega_1}(x)$.

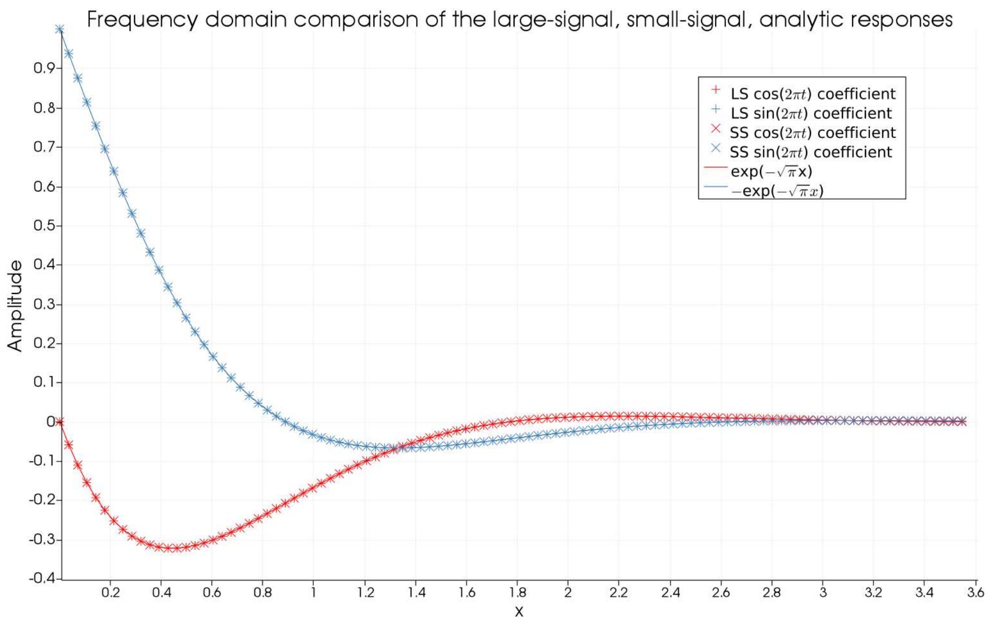

Figure 1: Plot of $U^C_{\omega_1}(x)$ and $U^S_{\omega_1}(x)$ as determined by the large-signal analysis (+,+), by the small-signal analysis (×, ×), and analytically (−, −).

At this scale, the three plotted responses are indistinguishable. We remark that the $\cos(0 \cdot 2\pi t)$ coefficient, i.e., the DC offset, exists on the order of 10^{-13} in these analyses. Of course, this term identically vanishes in the analytic solution.

4.2 Analysis of a non-linear perturbation

We now turn to a large-signal simulation of a sequence of non-linear perturbations of the Helmholtz equation from the previous section. Consider the PDE

$$\frac{\partial u}{\partial t} = u_{xx} - \epsilon \cdot u^2 \text{ on the domain } [0,1] \times \mathbb{S}^1$$

with mixed Dirichlet/Neumann boundary conditions

$$\begin{aligned} u(0,t) &= 3 \\ &\quad + 5\cos(2\cdot 2\pi t) + 5\sin(2\cdot 2\pi t) \\ &\quad - 4\cos(3\cdot 2\pi t) - 4\sin(3\cdot 2\pi t) \\ \frac{\partial u}{\partial x}(1,t) &= 0 \end{aligned}$$

for increasing values 0.0, 0.3, 0.6, 0.9, 1.2 and 1.5 of ϵ. Note that the PDE with $\epsilon = 0.0$ is identical to the linear Helmholtz equation of the previous section. Here, $\vec{\omega} = (\omega_1, \omega_2) = (2Hz, 3Hz)$.

Our results were obtained with a 2^{nd}-order box truncation scheme

$$\mathcal{T} := \{\vec{c} = (c_1, c_2) | 0 \le ||\vec{c}||_{\ell^a} \le 2\}.$$

In any truncation scheme, the stimuli tones correspond to the coefficient vectors of unit ℓ^1-norm:

$$\begin{aligned} 2Hz &= (+1, \quad 0)\cdot(2Hz, 3Hz) \\ 3Hz &= (\quad 0, +1)\cdot(2Hz, 3Hz) \end{aligned}$$

In Figure 2, we depict the cosine components of the solution, $U^C_{\omega_1}(x)$ and $U^C_{\omega_2}(x)$, as ϵ varies. Observe that the response at these stimulus frequencies does not change substantially.

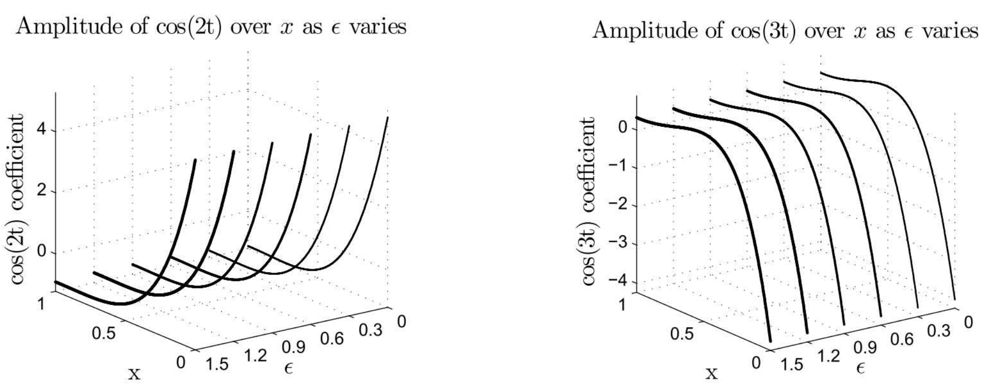

Figure 2: Cosine components of the response at the stimulus frequencies $2Hz$ and $3Hz$

In Figure 3, we plot the amplitudes of the cosine components at the $0, 1, 4$ and $5Hz$ frequencies. These frequencies lie at integer linear combinations of the stimulus frequencies corresponding to coefficient vectors of non-unit norm. This is reflected in our truncation scheme as:

$$1Hz = (-1,+1) \cdot (2Hz,3Hz) \qquad 4Hz = (+2,\ \ 0) \cdot (2Hz,3Hz)$$

$$5Hz = (+1,+1) \cdot (2Hz,3Hz) \qquad 6Hz = (\ \ 0,+2) \cdot (2Hz,3Hz)$$

The second-order tones, arising from second-order interactions, correspond to the coefficient vectors with ℓ^1-norm equal to 2. In particular, the 1,4, and $5Hz$ frequencies correspond to second-order interactions, and are not captured by the small-signal analysis. This phenomenon is reflected in the zero amplitude of the $\epsilon = 0$ curves in Figure 3, since $\epsilon = 0$ yields a linear system *devoid of non-linear terms*. As ϵ increases, the effect of non-linearity in the system increases the amplitudes of these second-order terms.

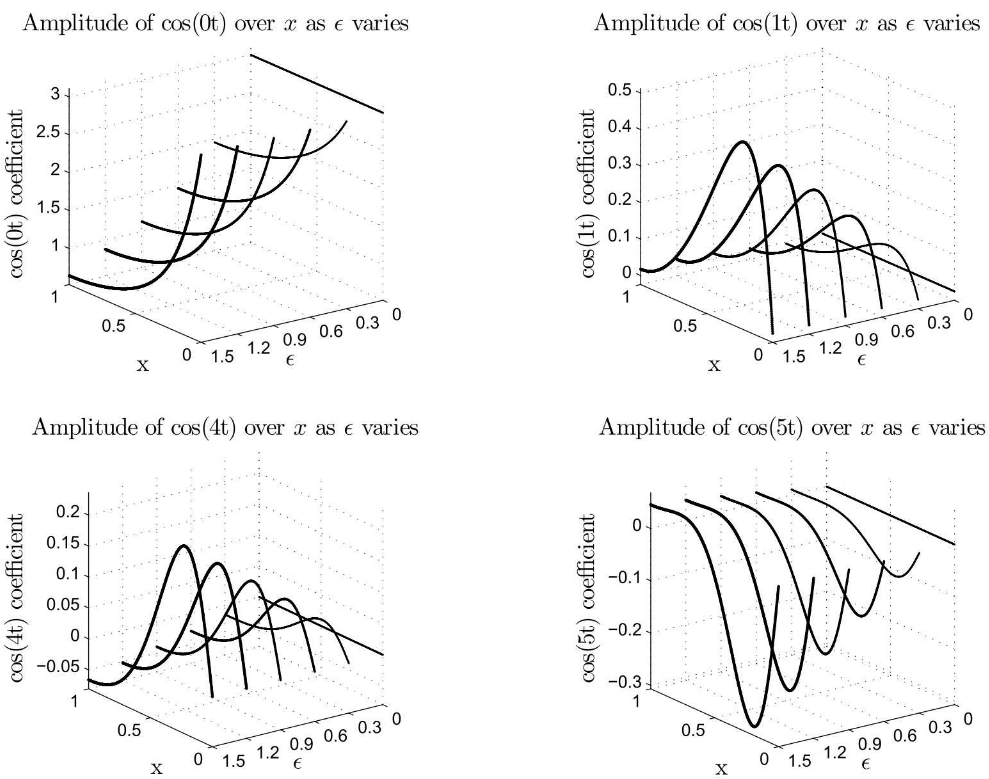

Figure 3: Cosine components of the Fourier series of the cross-terms

DISTRIBUTION:

1	MS	1177	Joseph Castro, 01355
1	MS	1177	Xujiao (Suzey) Gao, 01355
1	MS	1177	Gary Hennigan, 01355
1	MS	1177	Lawrence C. Musson, 01355
1	MS	1177	Mihai Negoita, 01355
1	MS	1177	Heidi K. Thornquist, 01355
1	MS	1318	Roger P. Pawlowski, 01446
1	MS	1318	Kara J. Peterson, 01442
1	MS	1318	Eric T. Phipps, 01441
1	MS	1320	Eric C. Cyr, 01442
1	MS	1321	Jason M. Gates, 01442
1	MS	0899	Technical Library, 9536 (electronic copy)

This page intentionally left blank.

Sandia National Laboratories